

# Demystifying the role of sintering additives with “complexion”

Shen J. Dillon, Martin P. Harmer\*

Center for Advanced Materials and Nanotechnology, Lehigh University, 5 East Packer Avenue, Bethlehem, PA 18015, United States

Available online 18 January 2008

## Abstract

The role of additives has long been a theme in sintering science. Recently, it has been discovered that ceramics may contain multiple different grain boundary phases (complexions) that are chemically induced by certain additives. These complexions are useful in explaining a number of anomalous phenomena associated with sintering, such as abnormal grain growth. The current work investigates how transitions between these complexions occur and at which grain boundaries they are most likely to occur. The number of complexion transitions that occur increases linearly with grain size (grain boundary excess concentration), and exponentially with temperature. The results suggest that grain boundary energy and anisotropy are important in predicting which and how many grain boundaries will undergo such a transition.

© 2007 Elsevier Ltd. All rights reserved.

**Keywords:** Grain growth;  $\text{Al}_2\text{O}_3$ ; Grain boundaries; Sintering

## 1. Introduction

The use of sintering additives has been an effective strategy for microstructure control in ceramics. Sir Richard J. Brook performed early pioneering work on both microstructural evolution during sintering, and the optimization of processing and microstructures through the use of additives.<sup>1–16</sup> Prof. Brook's classic work on modeling pore–boundary interactions is a mainstay of sintering and grain growth textbooks.<sup>17</sup> Brook maps<sup>17</sup> have provided an easy and convenient way of visualizing a complex problem. His insight into the subject focused our attention on important ratios; the ratio of the pore to boundary mobility,<sup>17</sup> the ratio of diffusional pre-exponential to activation energy,<sup>18</sup> and the ratio of the relative densification rate to the relative grain growth rate.<sup>19–22</sup> He was the first to recognize the effect of solute drag on the grain growth exponent and its critical effect on microstructural evolution in ceramics.<sup>23</sup> He was helpful in guiding researchers in the field to appreciate the complexity of the sintering problem.<sup>21,24–27</sup> Much of this is well described in his classic review paper on controlled grain growth.<sup>28</sup> He made many important contributions by designing and implementing critical experiments.<sup>8,21,29,30</sup> Of particular note, was his proposed strategy to use hot pressing as a means to study densification without grain growth.<sup>21</sup> He introduced the con-

cept of fast firing as a new processing strategy that has become widely established as an effective approach for producing dense fine-grained ceramics by pressure-less sintering.<sup>19,20</sup> In addition to basic science, he also contributed to developing a number of novel ceramic processing techniques.<sup>31–36</sup>

Despite much progress, however, fundamental mechanisms are still debated even after 50 years of continuous study.<sup>37</sup> Two examples of this are the mechanism(s) for abnormal grain growth, and the classic debate over the role of magnesia as a sintering aid.<sup>37–39</sup> However, the recent discovery of interface “complexions” offers a new perspective and possible solution to such problems.<sup>40,41</sup>

Interface complexions are equilibrium interface ‘phases’ that have associated thermodynamic properties.<sup>41</sup> Interface complexions have some characteristic equilibrium feature such as; a characteristic solute profile, a crystallographic reconstruction, a common disorder parameter, interfacial film width, etc. Thermodynamics predict that their stability is dependent on temperature, chemistry, and crystallography.<sup>41–44</sup> The well-documented intergranular films in materials such as silicon nitride and silicon carbide are one example of a grain boundary complexion.<sup>45–48</sup> Similar interface complexions have also been observed in zinc oxide,<sup>49</sup> silicon nitride,<sup>50</sup> olivine,<sup>51</sup> silicon carbide,<sup>52</sup> alumina,<sup>53</sup> ruthenates,<sup>54</sup> strontium titanate,<sup>55</sup> barium titanate,<sup>56</sup> aluminum nitride,<sup>57</sup> metal–ceramic interfaces,<sup>58,59</sup> and a nickel–tungsten alloy.<sup>60</sup> Recent work by the authors has shown that six distinctly different grain boundary complexions may exist in alumina, and that several grain boundary complex-

\* Corresponding author. Tel.: +1 610 758 4227; fax: +1 610 758 4244.  
E-mail address: [mph2@lehigh.edu](mailto:mph2@lehigh.edu) (M.P. Harmer).

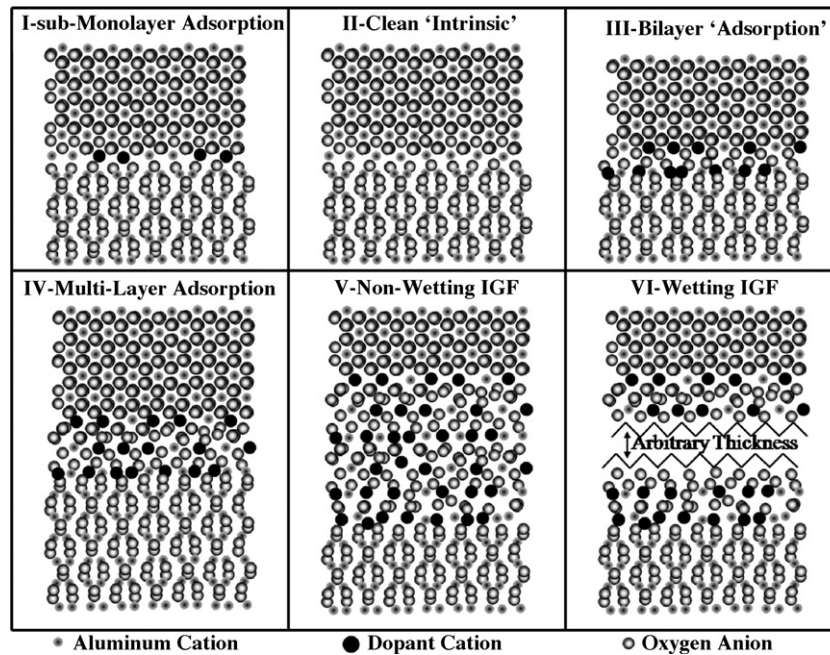


Fig. 1. Schematic of the six different grain boundary complexes observed in alumina. These include: submonolayer adsorption, a 'clean' boundary, bilayer adsorption, multilayer adsorption, a non-wetting intergranular film (IGF), and a wetting IGF.

ions may coexist in the same microstructure.<sup>40,41</sup> These grain boundary complexes in alumina are submonolayer adsorption, the clean 'intrinsic' boundary, bilayer adsorption, multilayer adsorption, a non-wetting intergranular film (IGF), and a wetting intergranular film.<sup>41</sup> These six boundaries are listed in order of increasing grain boundary mobility, and are shown schematically in Fig. 1. Each grain boundary complex has its own associated characteristic average grain boundary mobility (absent significant second-phase drag effects<sup>61–63</sup>), and there is a trend of increasing mobility with increasing disorder within the core of the grain boundary. The coexistence of any two or more complexes within a microstructure is the condition for abnormal grain growth. Certain dopants promote the coexistence of multiple complexes and high mobility complexes, while others stabilize low mobility complexes. The role of magnesia in preventing abnormal grain growth in alumina is to stabilize a single low mobility complex.<sup>41</sup> In this sense, understanding grain boundary complexes helps to simplify a complex problem. However, it is still not clear how, why and under what conditions *transitions* between different complexes occur.

Prof. Brook was also one of the first researchers to recognize the role of inhomogeneities in the sintering process, and treat them quantitatively.<sup>27,64</sup> Since early work on the subject, abnormal grain growth in alumina has often been attributed to inhomogeneities.<sup>65</sup> There are two principal kinds of inhomogeneities that may exist in a green or sintered body; extrinsic and intrinsic. Extrinsic inhomogeneities are associated with imperfect processing. Poor mixing, chemical segregation during drying, agglomeration, or defects in powder consolidation are examples of cases where inhomogeneities may arise. Intrinsic inhomogeneities are associated with anisotropy in the material.<sup>66</sup>

It has been shown that an inhomogeneous distribution of impurities or dopants in alumina would produce abnormal grains growing where the chemical composition was highest.<sup>67,68</sup> A number of researchers have observed qualitatively that increasing dopant concentration increases the volume fraction of abnormal grains in alumina.<sup>69–72</sup> Some have suggested that there is some 'critical concentration' above which a grain boundary

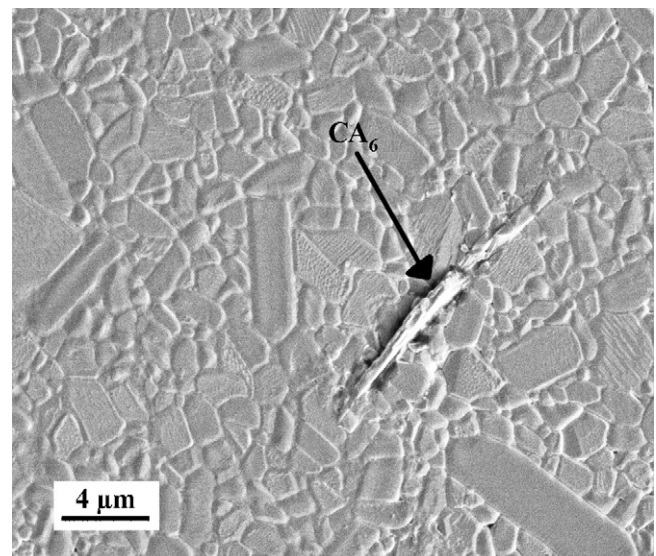


Fig. 2. SEM micrograph of 100 ppm calcia-doped alumina showing a second-phase calcium hexaluminate particle marked by an arrow. All the grain boundaries in contact with this particle will be saturated with calcium, and none of them have become abnormal. However, there are other abnormal grains in the microstructure that are not associated with any visible second phase. This indicates that the presence of a saturated boundary alone will not produce abnormal grain growth in alumina.

always becomes abnormal.<sup>73,74</sup> It is not surprising then that regions of the material with the highest levels of dopant or impurities may show complexion transitions and abnormal grain growth first.<sup>40</sup> However, even when the concentration is high locally it is still questionable which particular grain boundary might undergo a structural transition necessary to produce abnormal grain growth. The cation diffusivity along a grain boundary of alumina is known to be orders of magnitude higher than its diffusivity across a grain boundary.<sup>75</sup> It is possible that at high temperatures cations segregated to the grain boundaries may be able to redistribute themselves locally, to some extent. Fig. 2 illustrates the difficulty in trying to predict exactly which grain boundaries will become abnormal based solely on considerations of dopant level. In this figure, there is a large calcium hexaluminate second-phase particle (indicated by the arrow) surrounded by normal grains. The grain boundaries of all of these grains should be saturated with calcium, assuming they are in equilibrium with the precipitate they are in contact with. In fact, in order for the precipitate to grow to this size calcium had to dif-

fuse along the grain boundaries of the adjacent alumina grains. While the boundaries of these grains are saturated and have not become abnormal, there are abnormal grains nearby in the microstructure that are not in contact with second phase. While there may be unseen second phase below the surface of the sample, it still does not discount the fact that some saturated grain boundaries do not become abnormal while other saturated grain boundaries do. This figure suggests that inhomogeneities introduced during processing (extrinsic) may not be the only factor affecting complexion transitions. The intrinsic inhomogeneity may play an important role in affecting the local chemistry and grain boundary complexion transition.

Because the presence of abnormal grains and their kinetics are so intimately associated with their particular grain boundary complexion,<sup>41</sup> it is possible to study the distribution of grain boundary complexions in a microstructure by monitoring the distribution of abnormal grains. A quantitative description of this distribution with sintering time, grain size, dopant composition, dopant species, and temperature may provide insight into

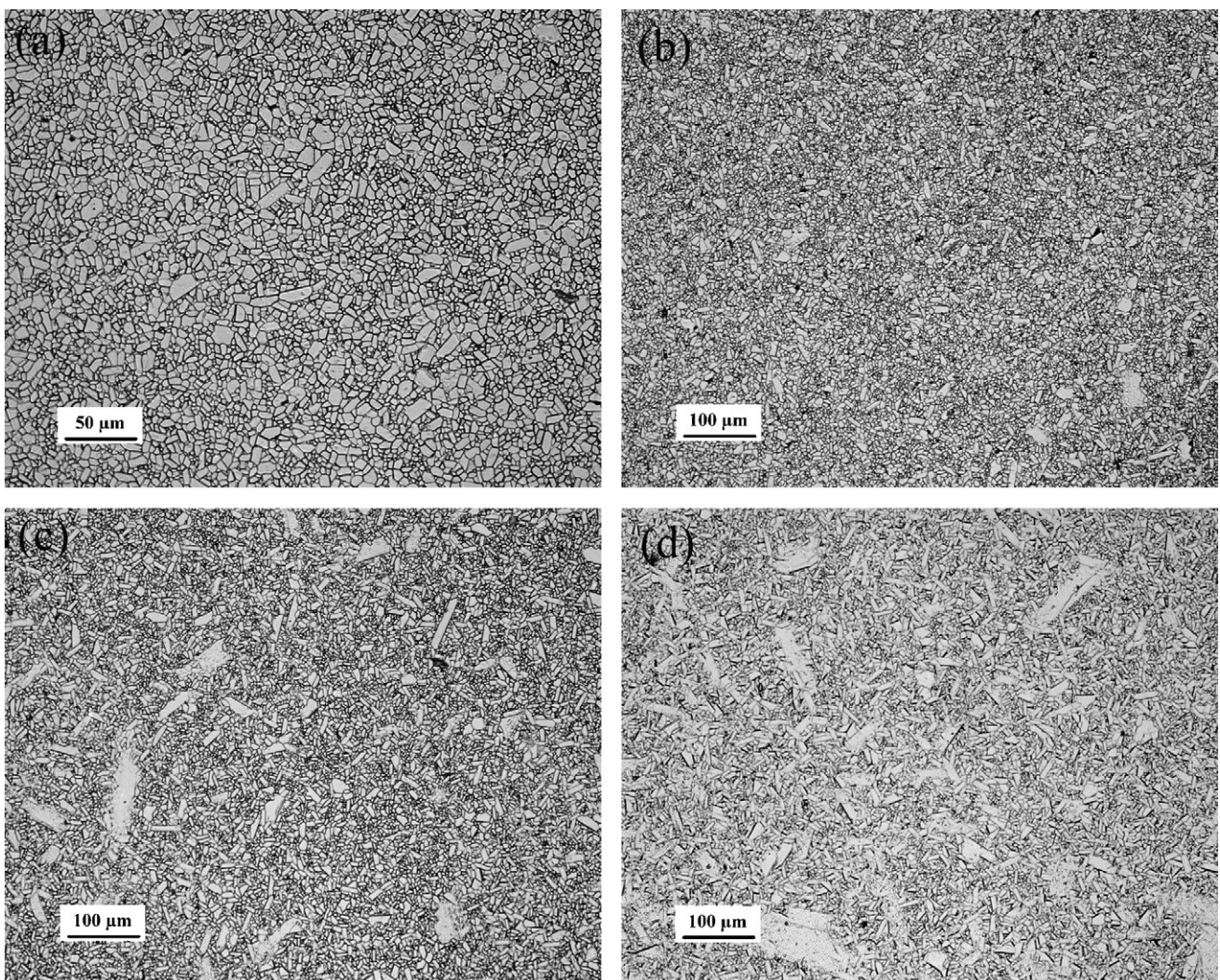


Fig. 3. Representative optical micrographs of 30 ppm calcia-doped alumina grown to equivalent normal grain size (9  $\mu\text{m}$ ) at (a) 1400  $^{\circ}\text{C}$ , (b) 1475  $^{\circ}\text{C}$ , (c) 1550  $^{\circ}\text{C}$ , and (d) 1625  $^{\circ}\text{C}$ .

understanding which grains are likely to undergo a complexion transition (i.e. abnormal grain growth). This paper attempts to quantitatively understand transitions between complexions, the cause of these transitions, and their relation to inhomogeneities. We hope this work adds insight into a field that Prof. Brook has made great contributions to, and carries on his themes of understanding the role of additives, inhomogeneities, and providing simplification of a complex problem.

## 2. Experimental procedure

Silica ( $\text{SiO}_2$ ) doped alumina ( $\alpha\text{-Al}_2\text{O}_3$ ) samples were prepared in nominal composition of 200 ppm. Alumina powder (Sumitomo, AKP-50 99.995%, Sumitomo Chemical, Tokyo, Japan) was mixed with tetraethylorthosilicate (Alfa Aesar, Ward Hill, MA) in methanol, dried and calcined. Calcia (CaO) doped alumina samples were prepared in the nominal compositions of 30 and 100 ppm. Alumina powder was mixed with calcium nitrate ( $\text{Ca}(\text{NO}_3)_2 \cdot 4\text{H}_2\text{O}$ ) (Alfa Aesar Puratronic 99.9995%, Alfa Aesar) in alcohol, dried, and subsequently calcined. All powders were processed in a class 1000 clean room in acid washed polytetrafluoroethylene and polyethylene containers. Samples were hot pressed at 50 MPa, for 2 h at 1300 °C (Astro 1000, Thermal Technology Inc., Santa Rosa, CA). Samples were annealed at temperatures ranging from 1325 to 1675 °C (Centorr S15, Centorr Vacuum Industries, Nashua, NH). Grain growth data from a previous study was used to calculate sintering times for calcia-doped alumina that would produce an equivalent normal grain size in each sample at different temperatures.<sup>61</sup> 30 ppm calcia-doped alumina was annealed to produce a normal grain size of 9  $\mu\text{m}$ , and 100 ppm calcia-doped alumina was sintered to produce a grain size of 3.5  $\mu\text{m}$ . This was done so that samples at different temperatures would have an equivalent grain boundary excess composition of calcia (neglecting the weak temperature dependence of solubility in alumina). Previous studies have shown that unimpinged abnormal grain boundaries separate from second-phase particles and excess solute leaving them entrapped within the abnormal grain, rather than pushing it in front of the grain. This indicates that the equivalent grain boundary excess concentration for equivalent normal grain size will be valid regardless of the volume fraction of abnormal grains. Other samples were annealed for various times to determine the number density of abnormal grains as a function of grain size. Heating and cooling rates of 100 °C/min were used. Ten low magnification images were taken randomly using a light optical microscope. The number of abnormal grains in each image was counted by hand. Measurements of normal grain size were performed using the linear intercept method.

Electron back scatter diffraction (EBSD) was performed in the FEI XL30 using the TSL system which included a digiview camera and the OIM data collection software (TexSEM, EDAX, Mahwah, NJ). EBSD was performed at 20 kV with the sample tilted to 70°. Samples for the transmission electron microscopy (TEM) (Jeol 2200FS, Jeol USA Inc., Peabody, MA) were prepared using a focused-ion beam microscope (FEI DB235, FEI Company, Hillsboro, Oregon).

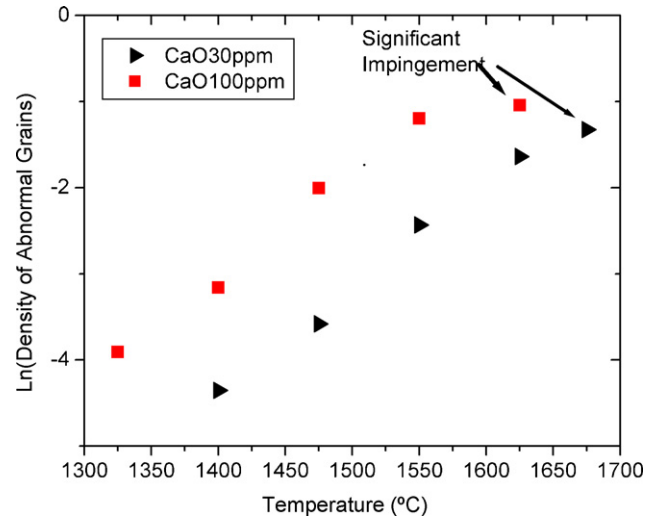


Fig. 4. Plot of the number density of abnormal grains versus temperature for two different constant excess grain boundary compositions in alumina doped with different levels of calcia, which shows an exponential dependence. These samples had an average grain size of 3 and 9  $\mu\text{m}$  for the 30 and 100 ppm calcia-doped samples, respectively.

## 3. Results and discussion

Representative microstructures of 30 ppm calcia-doped alumina are shown in Fig. 3. Fig. 4 shows the number density of abnormal grains for two different constant excess grain boundary compositions (i.e. equivalent average normal grain sizes) in alumina doped with different levels of calcia. The solubility of calcia in alumina is thought to be near 30 ppm so the excess grain boundary composition in this alumina should be much less than that of the 100 ppm calcia-doped alumina. This is reflected in the fact that the number density of abnormal grains in the 100 ppm calcia-doped alumina is always higher for any given temperature. The density of abnormal grains increases exponentially with increasing temperature up until the point of impingement.

The increase in the number density of abnormal grains is linear with grain size (Fig. 5). The number density was normalized by dividing the measured density by the average volume of the abnormal grain. This was done to account for stereological considerations about the probability of cross-sectioning through a

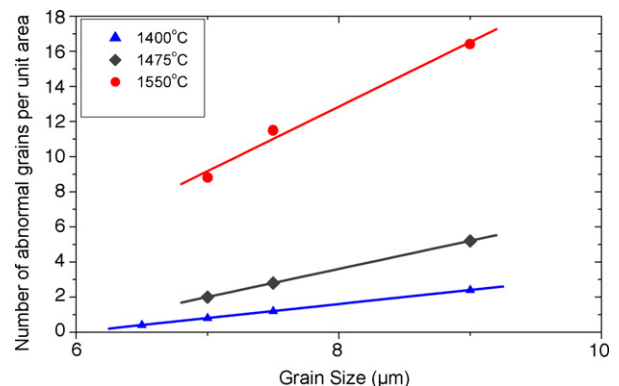


Fig. 5. Plot of the number density of abnormal grains versus grain size, which shows a linear dependence.

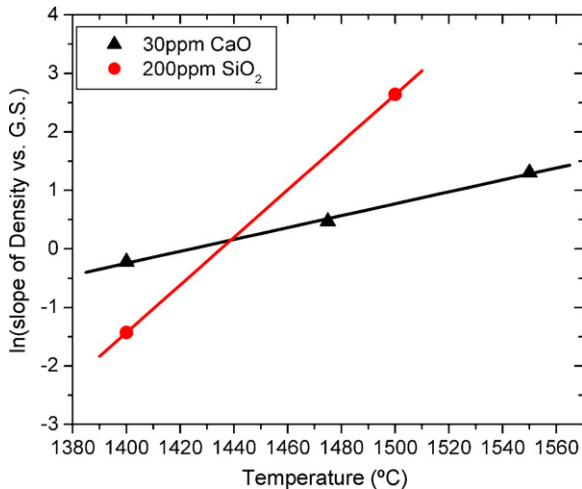


Fig. 6. Plot of the slope of each line of number density versus grain size (Fig. 5) versus temperature, for 200 ppm silica-doped alumina and 30 ppm calcia-doped alumina.

particular grain. The slope of each line of number density versus grain size increases exponentially with increasing temperature, as shown in Fig. 6. The slope of the line for calcia-doped alumina in this figure is in agreement, within error, with the slope of the line in Fig. 4. The grain boundary excess composition is directly proportional to the grain size up to the grain boundary saturation limit. This indicates there is a general trend in the data that the number density of abnormal grains increases linearly with increasing grain boundary excess concentration and exponentially with temperature for any particular grain boundary excess concentration.

For any particular grain boundary there is some level of excess dopant concentration necessary to induce a transition. It is known that pure undoped alumina does not undergo any complexion transitions up to 99% of the melting temperature.<sup>75</sup> As the grain size increases the grain boundary excess increases, which increase the probability that some individual grain boundary will reach the level of excess necessary to induce a transition. This explains the linear relationship between the number density of abnormal grains and the grain size. However, for some grain boundaries the grain boundary excess level required to induce a transition may be above the saturation limit and a precipitate will form before a transition may occur.

The idea that a ‘critical concentration’ is the only criterion for a grain boundary transition and abnormal grain growth is proved false by the temperature dependence of the number density of abnormal grains. If there were a critical concentration then the number density of abnormal grains would be constant for a constant grain boundary excess concentration, regardless of the temperature.

The results also contradict a theory that has grown in popularity lately, that abnormal grain growth in alumina, doped in the parts/million levels, is nucleation limited interface controlled.<sup>38</sup> The theory does not predict such a temperature dependence or grain size dependence of the number density of abnormal grains. The current authors have previously shown theoretically that nucleation limited interface controlled abnormal grain

growth theory may not be applied to single phase and pseudo-single phase alumina.<sup>39</sup> The current experimental evidence along with other experimental evidence further discounts the theory.

The activation energy for the transitions is 1002 and 257 kJ/mol for silica-doped alumina and calcia-doped alumina, respectively. The underlying source of this apparent activation energy is not obvious. There are two factors that may affect the measured activation energy for a grain boundary complexion transition. There is the activation energy barrier associated with the grain boundary transitioning from one stable state to another through some intermediate state ( $\Delta E$ ), and there is the temperature dependence of the free energy of the two different complexions that describes which is more stable (which results from temperature dependence of  $\Delta G$ ). This is shown schematically in Fig. 7. The thermodynamics of such a transition have been described theoretically by Tang et al.,<sup>42–44</sup> based on a modification of Cahn’s critical point wetting theory.<sup>76</sup> They predict that for any particular temperature the likelihood of a grain boundary transition increases with increasing misorientation and dopant concentration. They also predict that for a particular dopant concentration the lower misorientation boundaries will transition at higher temperatures and vice versa.<sup>42–44</sup> It may be more general to consider grain boundary energy rather than misorientation because the inclination of the grain boundary plane is likely to be a critical factor.<sup>66,77</sup> In this case, the likelihood of a transition should increase with increasing grain boundary energy. Saylor et al.<sup>78</sup> have shown experimentally that the density of boundaries of a particular energy increases exponentially with decreasing grain boundary energy. The work of Tang et al.<sup>42</sup> and Saylor et al.<sup>78</sup> predicts exactly what we see experimentally, that the number of abnormal grains will increase exponentially with increasing temperature. At any particular temperature, there may be a grain boundary energy above which all boundaries having those energies will go through a transition. This is shown schematically in Fig. 8, where  $T_2 > T_1$  and that the number of grain boundaries that undergo a transition is equivalent to the area under the curve. Similar ideas have been proposed for the effect of anisotropy on wetting.<sup>79</sup> The idea that the probability of a grain boundary transition is intimately related to its grain boundary energy is supported by evidence from previous studies such as; low energy basal planes are the least likely to undergo a transition in calcia-doped alumina,<sup>61</sup> and that low-energy bicrystal boundaries are less likely to transition than high-angle grain boundaries in real microstructures.<sup>80,81</sup> Several previous stud-

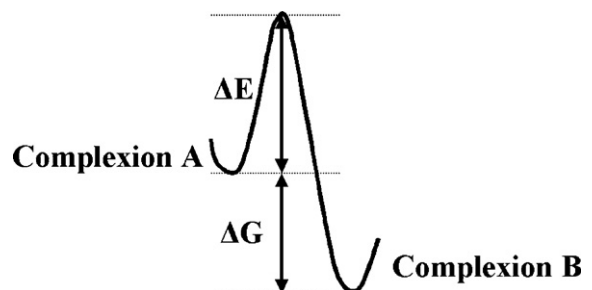


Fig. 7. Simple schematic of an energy barrier to a grain boundary transition.

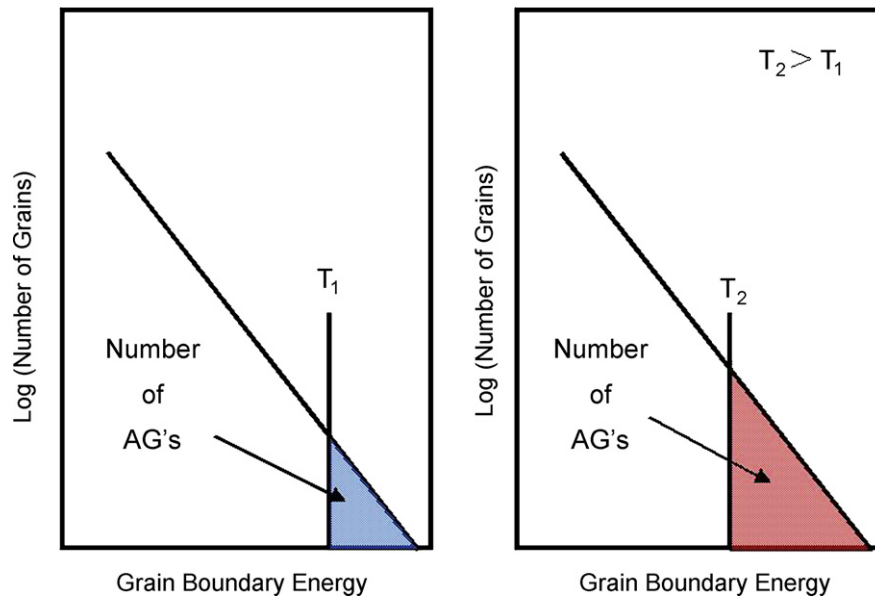


Fig. 8. Schematic showing how a linear increase in temperature produces an exponential increase in the number density of abnormal grains by decreasing the critical grain boundary energy necessary to produce a transition.

ies have shown that high-energy planes and grain boundaries show the highest levels of dopant segregation.<sup>66,82–84</sup> This effect also increases the likelihood of a grain boundary transition for high-energy grain boundaries relative to low energy grain boundaries. This suggests that intrinsic inhomogeneities in interfacial energy and dopant concentration at a particular boundary due to anisotropy are the major effect in complexion transitions.

However, it is known that after a grain boundary transition, a single abnormal grain samples various misorientations and grain boundary planes as it consumes multiple neighboring grains. The fact that an abnormal grain continues to grow after the initial grain boundary character is lost suggests that the true activation energy associated with transitioning from one complexion to another ( $\Delta E$ ) is not trivial. Small grains are often found entrapped within a large abnormal grain. EBSD indicates that these grains are low-angle misorientations or near coinci-

dent site lattice boundaries (Fig. 9a), and transmission electron microscopy indicates that the intergranular film associated with the abnormal growth of the large grain has dewet this entrapped grain (Fig. 9b). This result shows that it is possible for a grain boundary to transition back to its more ordered structure, but that the associated driving force (i.e. change in free energy) must be large. This is supported by previous results from Luo et al.<sup>85</sup> who showed that such a reverse transition took weeks to occur. A reverse transition may be less likely to occur because the higher concentration of solute in the more disordered boundary must be removed before such a transition may occur. This imposes a thermodynamic barrier to reverse transitions, in that there is an energy that must be overcome to either nucleate a precipitate or dissolve solute in the lattice above its solubility limit. This means that the activation energy associated with a reverse transition would be greater than that of the initial grain boundary

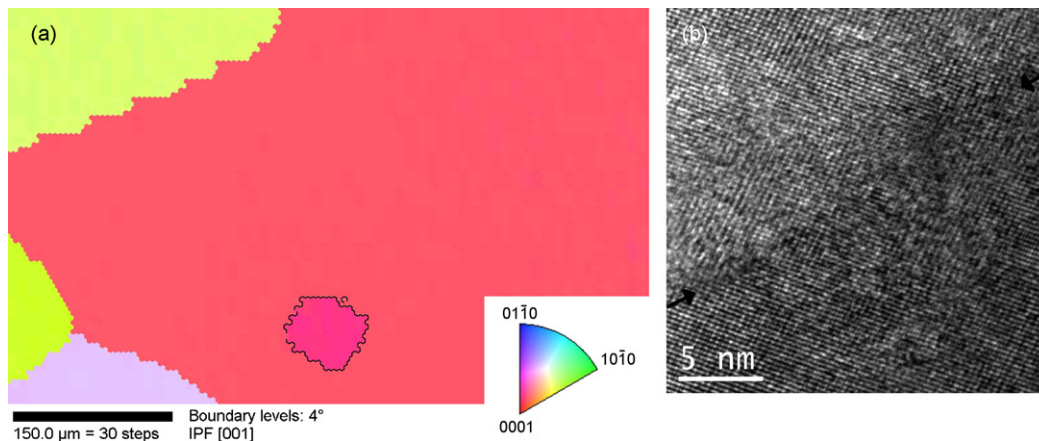


Fig. 9. (a) Orientation image maps of a small grain entrapped (outlined) in large abnormal grain. In (a) the entrapped grain is a low-angle boundary ( $\sim 4^\circ$ ). (b) HRTEM micrograph of a near  $\Sigma 1$  (low-angle) grain boundary, which shows no evidence of any intergranular film, which indicates that this boundary was dewetted by the film on the abnormal grain. The boundary is indicated by the arrows, and is difficult to see because it is a low-angle boundary.

complexion transition. Either the precipitation or dissolution of the excess solute is also kinetically limited processes. The time it takes them to occur may be longer than the time it takes to grow through a grain that forms an unstable boundary with the growing abnormal grain. This suggests that the abnormal grains may be metastable due to thermodynamic and kinetic limitations. Additionally, there is no theoretical explanation as to why the energy barrier ( $\Delta E$ ) to a grain boundary transition would be as significantly different for different chemistries as the measured activation energies for silica- and calcia-doped alumina. While the valence is different, it might be expected that calcia, which is the larger cation, might produce a larger energy barrier to a transition. Both boundaries have similar mobilities, so it is not expected that the diffusivity of either species in the alumina grain boundary would be significantly different. This suggests that the energy barrier ( $\Delta E$ ) is not controlling the measured activation energy. In all, it is inferred that while the true activation energy associated with the energy barrier to a grain boundary transition ( $\Delta E$ ) is non-trivial, the measured activation energy is more associated with the change in free energy between the initial and final state ( $\Delta G$ ) and the distribution of grain boundary energies.

It has long been known that dopants in alumina have an effect on the distribution of grain boundary energies. Most notably magnesia is well known to decrease the energy of all boundaries and produce a more isotropic distribution.<sup>82,86</sup> This decrease in grain boundary energy might also explain why magnesia-doping suppresses grain boundary transitions and prevents abnormal grain growth in alumina. The measured temperature dependence of the number density of abnormal grains may be somewhat representative of the distribution of grain boundary energies and might be correlated with measures of the grain boundary character distribution.

For a typical type of abnormal grain that is 10 times the size of the normal grains, only 0.1% of the grains must become abnormal for the microstructure to be completely consumed by abnormal grains. When the number density of abnormal grains is 0.01% they are not very significant in the measure of an average grain size, but a factor of 10 increase in the number density produces a complete transition of the whole microstructure. With a high activation exponential such as the one observed for silica-doped alumina, it appears that the transition occurs at some 'critical temperature'. Such a critical temperature has been observed in previous studies, but is likely due to a similar exponential behavior. The number of grains that undergo a transition in a typical microstructure that contains the occasional abnormal grain may be on the order of 1 in 10,000 to 1 in 1,000,000. The nucleation of a single abnormal grain for single crystal conversion,<sup>87</sup> as has been demonstrated previously, is literally a 1 in a billion event.<sup>88</sup> This indicates that the formation of an abnormal grain is a rather rare event, even when they are present throughout the microstructure. The seven degrees (5 macroscopic +2 microscopic) of freedom of the grain boundaries allow for the possibility of a large number of distinct grain boundaries. Because the temperature dependence of the density of abnormal grains fits exponential behavior there is some probability that an abnormal grain may form even at very low temperatures. Prac-

tically, the lower limit of temperature at which any abnormal grain may form is then determined by the energy of the highest energy grain boundary possible. Understanding this lower limit is of particular importance in applications where the presence of a single abnormal grain or high diffusivity complexion is not acceptable. A technologically significant example of this is in thermally grown alumina oxide scales on high-temperature superalloys in turbine engines.<sup>89</sup> Here a single complexion transition may produce a locally high oxidation rate, introducing a locally high growth stress, and cause spalling.

In order to achieve the level of microstructural control required to reproducibly induce a 1 in a billion event, it is critical to understand the influence of chemistry on the distribution of grain boundary energies. To design a toughened microstructure where there are large plate-like abnormal grains dispersed amongst small normal grains, it is necessary to select a dopant that produces a very anisotropic grain boundary energy distribution, which will promote anisotropic grain growth and produce a low apparent activation energy for the number density of abnormal grains that will allow normal and abnormal grains to coexist over a wide temperature range. In order to suppress grain boundary transitions all together it is important to select a dopant that lowers the energy of all of the grain boundaries. However, if it is only important to achieve a unimodal grain size distribution than it is sufficient to choose a dopant that promotes grain boundary isotropy. This ability to predict and control transitions between different grain boundary complexions through the use of chemistry and temperature is the foundation of kinetic engineering of materials. Our goal of understanding the effects of temperature and chemistry on processing materials is in the tradition and spirit of Sir Richard J. Brook, and this paper is dedicated to him on the occasion of his 70th birthday.

#### 4. Conclusions

The number density of abnormal grains (i.e. complexion transitions) increases linearly with grain boundary excess dopant concentration, and exponentially with temperature. Both the distribution of chemistry and the distribution of grain boundary energies, due to anisotropy, are important in predicting which grain boundaries undergo a complexion transition. The results indicate that low energy grain boundaries are the least likely to undergo a disordering transition. High-energy grain boundaries are, then, most likely to undergo a disordering complexion transition. These disordered complexions may then be metastable, due to the presence of a high concentration of solute. The number of transitions that occur in a particular microstructure is typically low. The highest temperature at which no abnormal grains will form will be defined by the energy of the highest energy grain boundary.

#### References

1. Bowen, L. J., Carruthers, T. G. and Brook, R. J., Hot-pressing of silicon nitride with yttrium oxide and lithium oxide as additives. *Journal of the American Ceramic Society*, 1978, **61**, 335–339.
2. Brook, R. J., Effect of titanium dioxide on the initial sintering of aluminum oxide. *Journal of the American Ceramic Society*, 1972, **55**, 114–115.

3. Brook, R. J., Additives and the sintering of ceramics. *Science of Sintering*, 1988, **20**, 115–118.
4. Brook, R. J., Gilbert, E., Shaw, N. J. and Eisele, U., Solid solution additives and the sintering of ceramics. *Powder Metallurgy*, 1985, **28**, 105–107.
5. Brook, R. J., Yee, J. and Kroger, F. A., Electrochemical cells and electrical conduction of pure and doped aluminum oxide. *Journal of the American Ceramic Society*, 1971, **54**, 444–451.
6. Coble, R. L., Song, H., Brook, R. J., Handwerker, C. A. and Dynys, J. M., Sintering and grain growth in alumina and magnesia. *Advances in Ceramics*, 1984, **10**, 839–852.
7. Harmer, M., Roberts, E. W. and Brook, R. J., Rapid sintering of pure and doped  $\alpha$ -alumina. *Transactions and Journal of the British Ceramic Society*, 1979, **78**, 22–25.
8. Harmer, M. P. and Brook, R. J., The effect of magnesia additions on the kinetics of hot pressing in alumina. *Journal of Materials Science*, 1980, **15**, 3017–3024.
9. Howlett, S. P., Brook, R. J. and Gettings, M., Grain-boundary segregation of indium in cobalt monoxide. *Journal of Materials Science*, 1982, **17**, 3308–3316.
10. Kilner, J. A. and Brook, R. J., A study of oxygen ion conductivity in doped nonstoichiometric oxides. *Solid State Ionics*, 1982, **6**, 237–252.
11. Pickup, H. and Brook, R. J., Barium oxide as a sintering aid for silicon nitride. *British Ceramic Proceedings*, 1987, **39**, 69–76.
12. Xue, L. A., Chen, Y. and Brook, R. J., The influence of ionic radii on the incorporation of trivalent dopants into barium titanate ( $\text{BaTiO}_3$ ). *Materials Science & Engineering, B: Solid-State Materials for Advanced Technology*, 1988, **B1**, 193–201.
13. Xue, L. A., Chen, Y. and Brook, R. J., The effect of lanthanide contraction on grain growth in lanthanide-doped barium titanate ( $\text{BaTiO}_3$ ). *Journal of Materials Science Letters*, 1988, **7**, 1163–1165.
14. Xue, L. A., Chen, Y., Gilbert, E. and Brook, R. J., The kinetics of hot pressing for undoped and donor-doped barium titanate ( $\text{BaTiO}_3$ ) ceramics. *Journal of Materials Science*, 1990, **25**, 1423–1428.
15. Zhen, Y. S., Milne, S. J. and Brook, R. J., Oxygen ion conductivity of  $\text{La}_2\text{O}_3$  doped with alkaline earth oxides. *Materials Science Monographs*, 1987, **38B**, 1989–1997.
16. Zhen, Y. S., Milne, S. J. and Brook, R. J., Oxygen ion conduction in ceria ceramics simultaneously doped with gadolinia and yttria. *Science of Ceramics*, 1988, **14**, 1025–1030.
17. Brook, R. J., Pore-grain boundary interactions and grain growth. *Journal of the American Ceramic Society*, 1969, **52**, 56–57.
18. Dosdale, T. and Brook, R. J., Comparison of diffusion data and of activation energies. *Journal of the American Ceramic Society*, 1983, **66**, 392–395.
19. Harmer, M. P., Roberts, E. W. and Brook, R. J., Fast firing of alumina ceramics. *Materials Science Monographs*, 1980, **6**, 155–162.
20. Harmer, M. P. and Brook, R. J., Fast firing—microstructural benefits. *Transactions and Journal of the British Ceramic Society*, 1981, **80**, 147–149.
21. Eisele, U. and Brook, R. J., The value of kinetic studies for the determination of sintering mechanisms. In *Ceramic Powder Process Sciences, Proceedings of International Conference, 2nd*, 1989, pp. 673–679.
22. Brook, R. J., Pores and grain growth kinetics. *Journal of the American Ceramic Society*, 1969, **52**, 339–340.
23. Brook, R. J., Impurity-drag effect and grain growth kinetics. *Scripta Metallurgica*, 1968, **2**, 375–378.
24. Brook, R. J., Developments in the sintering of ceramics. *Science of Ceramics*, 1977, **9**, 57–66.
25. Song, H., Coble, R. L. and Brook, R. J., The applicability of Herring's scaling law to the sintering of powders. *Materials Science Research*, 1984, **16**, 63–79.
26. Brook, R. J., Ceramic microstructures: the art of the possible. *Materials Science Research*, 1987, **21**, 15–24.
27. Brook, R. J., Tuan, W. H. and Xue, L. A., Critical issues and future directions in sintering science. *Ceramic Transactions*, 1988, **1**, 811–823.
28. Brook, R. J., Controlled grain growth. *Treatise on Materials Science and Technology*, 1976, **9**, 331–364.
29. Bowen, L. J., Weston, R. J., Carruthers, T. G. and Brook, R. J., Mechanisms of densification during the pressure sintering of alpha-silicon nitride. *Ceramurgia International*, 1976, **2**, 173–176.
30. Rahaman, M. N., De Jonghe, L. C. and Brook, R. J., Effect of shear stress on sintering. *Journal of the American Ceramic Society*, 1986, **69**, 53–58.
31. Di Rupo, E., Anseau, M. R. and Brook, R. J., Reaction sintering: correlation between densification and reaction. *Journal of Materials Science*, 1979, **14**, 2924–2928.
32. Di Rupo, E., Carruthers, T. G. and Brook, R. J., Identification of stages in reactive hot-pressing. *Journal of the American Ceramic Society*, 1978, **61**, 468–469.
33. McMillan, S. M. and Brook, R. J., Synthesis of silicon carbide ceramics at low temperatures. *Ceramic Transactions*, 1995, **51**, 187–191.
34. Stedman, S. J., Evans, J. R. G., Brook, R. J. and Hoffmann, M. J., Anisotropic sintering shrinkage in injection-molded composite ceramics. *Journal of the European Ceramic Society*, 1993, **11**, 523–532.
35. Tuan, W. H. and Brook, R. J., The toughening of alumina with nickel inclusions. *Journal of the European Ceramic Society*, 1990, **6**, 31–37.
36. Walker, C. N., Borsa, C. E., Todd, R. I., Davidge, R. W. and Brook, R. J., Fabrication, characterization and properties of alumina matrix nanocomposites. *British Ceramic Proceedings*, 1994, **53**, 249–264.
37. Dillon, S. J. and Harmer, M. P., Comment on effect of interface structure on the microstructural evolution of ceramics. *Journal of the American Ceramic Society*, 2007, **90**, 2291.
38. Jo, W., Kim, D.-Y. and Hwang, N.-M., Effect of interface structure on the microstructural evolution of ceramics. *Journal of the American Ceramic Society*, 2006, **89**, 2369–2380.
39. Dillon, S. J. and Harmer, M. P., Diffusion controlled abnormal grain growth in ceramics. *Materials Science Forum*, 2007, **558–559**, 1227–1236.
40. Dillon, S. J. and Harmer, M. P., Multiple grain boundary transitions in ceramics: a case study in alumina. *Acta Materialia*, 2007, **55**, 5247–5254.
41. Dillon, S. J., Tang, M., Carter, W. C. and Harmer, M. P., Complexion: a new concept for kinetic engineering in materials science. *Acta Materialia*, 2007, **55**, 6208–6218.
42. Tang, M., Carter, W. C. and Cannon, R. M., Grain boundary transitions in binary alloys. *Physical Review Letters*, 2006, **97**, pp. 075502/075501–175502/075504.
43. Tang, M., Carter, W. C. and Cannon, R. M., Grain boundary order–disorder transitions. *Journal of Materials Science*, 2006, **41**, 7691–7695.
44. Tang, M., Carter, W. C. and Cannon, R. M., Diffuse interface model for structural transitions of grain boundaries. *Physical Review B: Condensed Matter and Materials Physics*, 2006, **73**, pp. 024102/024101–124102/024114.
45. Subramaniam, A., Koch, C. T., Cannon, R. M. and Rühle, M., Intergranular glassy films: an overview. *Materials Science & Engineering, A: Structural Materials: Properties, Microstructure and Processing*, 2006, **A422**, 3–18.
46. Gu, H., Pan, X., Tanaka, I., Cannon, R. M., Hoffmann, M. J., Muellejans, H. and Rühle, M., Structure and chemistry of intergranular films in Ca-doped  $\text{Si}_3\text{N}_4$ . *Materials Science Forum*, 1996, **207–209**, 729–732.
47. Clarke, D. R., On the detection of thin intergranular films by electron microscopy. *Ultramicroscopy*, 1979, **4**, 33–44.
48. Ritchie, R. O., Zhang, X. F. and de Jonghe, L. C., On the role of grain-boundary films in optimizing the mechanical properties of silicon carbide ceramics. *Materials Research Society Symposium Proceedings*, 2004, **819**, 3–14.
49. Chiang, Y. M., Wang, H. and Lee, J. R., HREM and STEM of intergranular films at zinc oxide varistor grain boundaries. *Journal of Microscopy (Oxford)*, 1998, **191**, 275–285.
50. Gu, H., Cannon, R. M. and Rühle, M., Composition and chemical width of ultrathin amorphous films at grain boundaries in silicon nitride. *Journal of Materials Research*, 1998, **13**, 376–387.
51. Wirth, R., Thin amorphous films (1–2 nm) at olivine grain boundaries in mantle xenoliths from San Carlos, Arizona. *Contributions to Mineralogy and Petrology*, 1996, **124**, 44–54.
52. Volz, E., Roosen, A., Wang, S. C. and Wei, W. C. J., Formation of intergranular amorphous films during the microstructural development of liquid phase sintered silicon carbide ceramics. *Journal of Materials Science*, 2004, **39**, 4095–4101.



53. Brydson, R. R., Chen, S.-C., Riley, F. L., Pan, S. M.-X. and Rühle, M., Microstructure and chemistry of intergranular glassy films in liquid-phase-sintered alumina. *Journal of the American Ceramic Society*, 1998, **81**, 369–379.
54. Chiang, Y.-M., Silverman, L. A., French, R. H. and Cannon, R. M., Thin glass film between ultrafine conductor particles in thick-film resistors. *Journal of the American Ceramic Society*, 1994, **77**, 1143–1152.
55. Chung, S.-Y. and Kang, S.-J. L., Intergranular amorphous films and dislocations-promoted grain growth in SrTiO<sub>3</sub>. *Acta Materialia*, 2003, **51**, 2345–2354.
56. Choi, S.-Y., Yoon, D.-Y. and Kang, S.-J. L., Kinetic formation and thickening of intergranular amorphous films at grain boundaries in barium titanate. *Acta Materialia*, 2004, **52**, 3721–3726.
57. Yoshioka, T., Makino, Y., Miyake, S. and Mori, H., Properties and microstructure of aluminum nitride sintered by millimeter-wave heating. *Journal of Alloys and Compounds*, 2006, **408–412**, 563–567.
58. Avishai, A., Scheu, C. and Kaplan, W. D., Intergranular films at metal–ceramic interfaces. Part I—interface structure and chemistry. *Acta Materialia*, 2005, **53**, 1559–1569.
59. Ning, X. G., Pan, J., Hu, K. Y. and Ye, H. Q., Structural characterization of the b-silicon nitride whisker-aluminum interfaces in a beta-Si<sub>3</sub>N<sub>4</sub> whisker-Al alloy 6061 composite material. *Philosophical Magazine A: Physics of Condensed Matter: Structure, Defects and Mechanical Properties*, 1992, **66**, 811–821.
60. Luo, J., Gupta, V. K., Yoon, D. H. and Meyer III, H. M., Segregation-induced grain boundary premelting in nickel-doped tungsten. *Applied Physics Letters*, 2005, **87**, pp. 231902/231901–1231902/231903.
61. Dillon, S. J. and Harmer, M. P., Relating grain boundary complexion to grain boundary kinetics I: calcia-doped alumina. *Journal of the American Ceramic Society*, submitted for publication.
62. Dillon, S. J. and Harmer, M. P., Relating grain boundary complexion to grain boundary kinetics II: silica-doped alumina. *Journal of the American Ceramic Society*, submitted for publication.
63. Dillon, S. J. and Harmer, M. P., An experimentally quantifiable solute drag factor. *Acta Materialia*, in press.
64. Tuan, W. H. and Brook, R. J., Sintering of heterogeneous ceramic compacts. Part 2. Zirconia-alumina. *Journal of Materials Science*, 1989, **24**, 1953–1958.
65. Bennison, S. J. and Harmer, M. P., A history of the role of magnesia in the sintering of  $\alpha$ -alumina. *Ceramic Transactions*, 1990, **7**, 13–49.
66. Pang, Y. and Wynblatt, P., Effects of Nb doping and segregation on the grain boundary plane distribution in TiO<sub>2</sub>. *Journal of the American Ceramic Society*, 2006, **89**, 666–671.
67. Sone, T.-W., Han, J.-H., Hong, S.-H. and Kim, D.-Y., Effect of surface impurities on the microstructure development during sintering of alumina. *Journal of the American Ceramic Society*, 2001, **84**, 1386–1388.
68. Cho, S.-J., Kim, K.-H., Kim, D.-J. and Yoon, K.-J., Abnormal grain growth at the interface of centrifugally cast alumina bilayer during sintering. *Journal of the American Ceramic Society*, 2000, **83**, 1773–1776.
69. Wang, C.-M., Chan, H. M. and Harmer, M. P., Effect of Nd<sub>2</sub>O<sub>3</sub> doping on the densification and abnormal grain growth behavior of high-purity alumina. *Journal of the American Ceramic Society*, 2004, **87**, 378–383.
70. Ahn, J. H., Lee, J.-H., Hong, S.-H., Hwang, N.-M. and Kim, D.-Y., Effect of the liquid-forming additive content on the kinetics of abnormal grain growth in alumina. *Journal of the American Ceramic Society*, 2003, **86**, 1421–1423.
71. Yoo, J. H., Nam, J. C. and Baik, S., Quantitative evaluation of glass-forming impurities in alumina: equivalent silica concentration (ESC). *Journal of the American Ceramic Society*, 1999, **82**, 2233–2238.
72. Altay, A. and Güllün, M. A., Microstructural evolution of calcium-doped-alumina. *Journal of the American Ceramic Society*, 2003, **86**, 623–629.
73. Jung, J. and Baik, S., Abnormal grain growth of alumina: CaO effect. *Journal of the American Ceramic Society*, 2003, **86**, 644–649.
74. Bae, I.-J. and Baik, S., Abnormal grain growth of alumina. *Journal of the American Ceramic Society*, 1997, **80**, 1149–1156.
75. Dillon, S. J. and Harmer, M. P., Intrinsic grain boundary mobility in alumina. *Journal of the American Ceramic Society*, 2006, **89**, 3885–3887.
76. Cahn, J. W., Critical point wetting. *Journal of Chemical Physics*, 1977, **66**, 3667–3672.
77. Wynblatt, P. and Takashima, M., Correlation of grain boundary character with wetting behavior. *Interface Science*, 2002, **9**, 265–273.
78. Saylor, D. M., Morawiec, A., Rohrer, G. S. and Distribution, Energies of grain boundaries in magnesia as a function of five degrees of freedom. *Journal of the American Ceramic Society*, 2002, **85**, 3081–3083.
79. Takashima, M., Wynblatt, P. and Adams, B. L., Correlation of grain boundary character with wetting behavior. *Interface Science*, 2000, **8**, 351–361.
80. Dillon, S. J. and Harmer, M. P., Direct observation of multilayer adsorption on alumina grain boundaries. *Journal of the American Ceramic Society*, 2007, **90**, 996–998.
81. Dillon, S. J. and Harmer, M. P., Relating grain boundary complexion to grain boundary kinetics III: neodymia-doped alumina. *Journal of the American Ceramic Society*, 2007.
82. Baik, S. and Moon, J. H., Effects of magnesium oxide on grain-boundary segregation of calcium during sintering of alumina. *Journal of the American Ceramic Society*, 1991, **74**, 819–822.
83. Baik, S. and White, C. L., Anisotropic calcium segregation to the surface of aluminum oxide. *Journal of the American Ceramic Society*, 1987, **70**, 682–688.
84. Mukhopadhyay, S. M., Jardine, A. P., Blakley, J. M. and Baik, S., Segregation of magnesium and calcium to the prismatic surface of magnesium-implanted sapphire. *Journal of the American Ceramic Society*, 1988, **71**, 358–362.
85. Luo, J., Chiang, Y.-M. and Cannon, R. M., Nanometer-thick surficial films in oxides as a case of prewetting. *Langmuir*, 2005, **21**, 7358–7365.
86. Handwerker, C. A., Dynys, J. M., Cannon, R. M. and Coble, R. L., Dihedral angles in magnesia and alumina: distributions from surface thermal grooves. *Journal of the American Ceramic Society*, 1990, **73**, 1371–1377.
87. Scott, C., Kaliszewski, M., Greskovich, C. and Levinson, L., Conversion of polycrystalline Al<sub>2</sub>O<sub>3</sub> into single-crystal sapphire by abnormal grain growth. *Journal of the American Ceramic Society*, 2002, **85**, 1275–1280.
88. Dillon, S. J. and Harmer, M. P., Mechanism of “solid-state” single-crystal conversion in alumina. *Journal of the American Ceramic Society*, 2007, **90**, 993–995.
89. Hou, P. Y., Impurity effects on alumina scale growth. *Journal of the American Ceramic Society*, 2003, **86**, 660–668.